HAIL GROWTH PROCESSES IN AN ALBERTA HAILSTORM

Dennis J. Musil   and   Paul L. Smith
Institute of Atmospheric Sciences
South Dakota School of Mines and Technology
501 East St. Joseph Street
Rapid City, South Dakota 57701-3995

Abstract. A series of observations inside an Alberta hailstorm was made with the T-28 armored research aircraft during the summer of 1985, as part of the Alberta Hail Project. An analysis of some of the characteristics of the hail size distributions in relation to other T-28 measurements showed many features similar to past T-28 observations. Most of the hail observed was falling through the -17°C penetration level, even in the updrafts. A preliminary assessment of the hail growth mechanisms in this storm shows that most of the hailstones were in a dry growth regime at the penetration level, but likely in wet growth lower down in the storm. Recirculation of hydrometeors probably played a significant role in the hail development.

1. INTRODUCTION

Past studies of cloud turrets (feeder clouds or new growth) surrounding Alberta hailstorms and of the accompanying hailfall distribution patterns on the ground suggest that the turrets represent a major source of hailstone embryos for the storms (e.g., Krauss and Marwitz, 1984). If the feeder clouds are the major source of embryos for a natural hailstorm, then it follows that a seeding treatment designed to intervene in the hail process should be applied to that cloud region. This was the basis for hailstorm seeding experiments during the last few years of the Alberta Hail Project (English, 1986; Humphries et al., 1987).

Accordingly, controlled cloud seeding experiments involving three aircraft, radar, and ground-based sampling systems were conducted in the summer of 1985 in an attempt to confirm whether the clouds in the new growth zone are the major source of embryos, as well as to document the effects of seeding with an ice nucleant in those clouds. Plans called for cloud physics measurements by a Conquest research aircraft to identify and follow the initial growth and movement of ensembles of precipitation particles originating in the new growth zone. The armored T-28 research aircraft (Johnson and Smith, 1980) was to document the continued growth of the particles into hailstones by penetrating through the feeder clouds and on into the main part of the hailstorm. The radar observations and time-resolved hailstone samples collected at the ground would provide further information about the evolution of the hailstones. The magnetic-particle tracer technique described by Knight et al. (1986) was also tried in an effort to obtain further information about hailstone embryo sources and trajectories.

A storm which occurred on 11 July 1985 provided the best data for a detailed analysis effort. Unfortunately, funds supporting the Alberta Hail Project were sharply cut not long after the end of the 1985 season, so no such analysis effort could be completed. Nevertheless, the four penetrations made by the T-28 provided a data set which permits a preliminary

assessment of the hail growth processes in this storm. The purpose of this paper is to describe some of the measurements by the T-28 in the context of inferences about the hail growth mechanisms. Oleskiw and English (1986) have also discussed this storm.

2. BRIEF DESCRIPTION OF THE STORM

A representative sounding and hodograph from Red Deer, Alberta, are shown in Fig. 1. Cloud base conditions are estimated to be near the LCL, at a temperature of about +8°C and corresponding to a potential wet bulb temperature of 20°C.
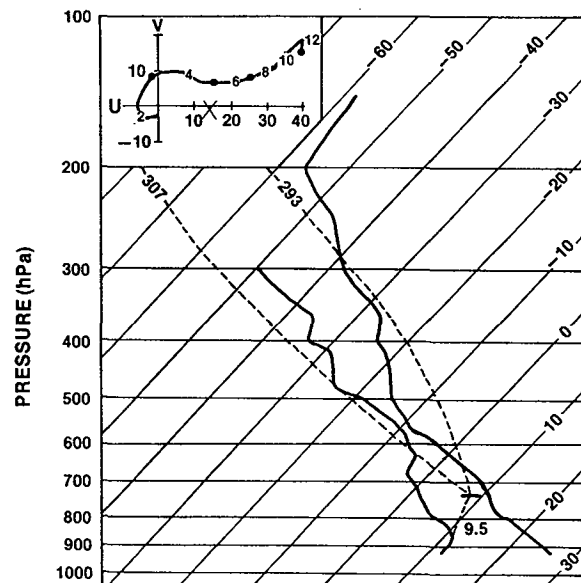
Fig. 1: Rawinsonde from Red Deer, Alberta at 2000 MDT on 11 July 1985 plotted on skew T-log P diagram. The LCL is located near +8°C and 735 hPa and is associated with a wet-bulb potential temperature of 20°C. The hodograph shown in the inset (wind components in m/s, heights in km) was derived from winds taken four hours earlier than the sounding plotted because of missing wind data at the later time. The storm motion is indicated by the X.

This indicates some negative thermal buoyancy in the updraft region at cloud base, with the level of free convection located near the 655 hPa level. The environmental wind shear from the estimated cloud base to the indicated top of the positive energy area was about 5.5×10^{-3} s^{-1}, while the sub-cloud environmental winds were weak and veered about 150° below the LCL. The hodograph is quite similar to that shown by Krauss and Marwitz (1984), except that the wind shear is somewhat stronger in this case.

The storm of interest formed well north of Red Deer and initially moved in a southerly direction, but then during the mature stage followed a path from west to east while producing up to walnut-sized hail. Its movement at about 14 m s^{-1} was well to the right of the mid-level winds, and it laid down a continuous hailswath over 200 km long. The storm was under study by project aircraft for over three hours, long enough for four different seeding treatments (including a placebo) to be applied in a randomized sequence (Oleskiw and English, 1986). Although the radar data have not been analyzed in great detail, the echo tops were around 11 km and the storm persistently had maximum reflectivity values >60 dBZ during the time of the research mission. A low elevation angle PPI representation of the storm near the time of the first T-28 penetration is shown in Fig. 2. It was fairly isolated with no visually distinct feeder clouds associated with the storm, according to personnel in the research aircraft. However, there were persistent cumulus towers growing on the south and west sides of the main storm, near the cloud-base feed-in area. Some of these towers extended 5-10 km from the parent cell and might be classified as feeder cells, although
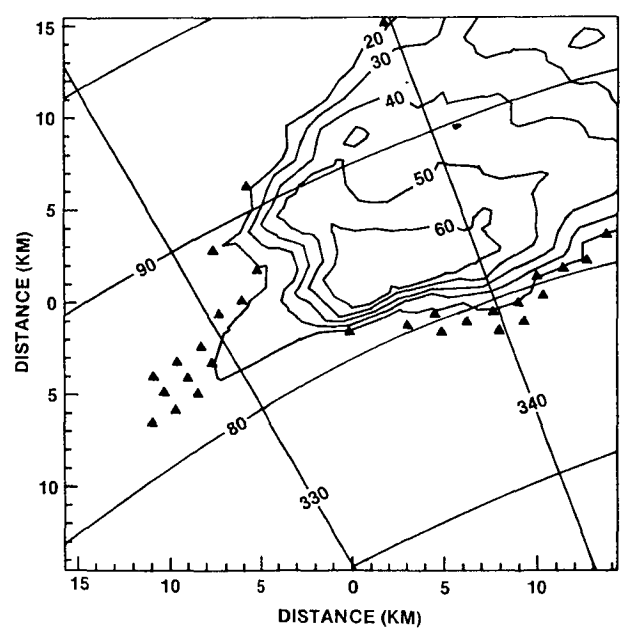
further analysis is required to verify that. The storm can best be classified as having very weak evolution (Foote and Frank, 1983), and probably had enough features to be called a "supercell."

3. SUMMARY OF T-28 PENETRATIONS

The T-28 made four penetrations of this storm; Table 1 shows the times of the penetrations and some of the pertinent observations from each. There was a break of approximately 30 minutes in the penetration sequence because of heavy icing encountered during the first two penetrations. The penetrations were all made at roughly the same average temperature of about -17°C, which corresponds to an altitude of about 6.2 km MSL.

	TIMES				VERTICAL DRAFTS				HAIL	
Pen	In	Out	L	θ_e	U	D	LWC	TURB	N_T	W_H*
	(MDT)		(km)	(K)	(m/s)		(g/m³)	(c$^{1/3}$)	(r^{-3})	(g/m³)
1	182942	183243	18.1	331	15	-10	2.4	15	8	12
2	183746	184135	22.9	329	6	-11	2.0	12	39	12
3	191421	191723	18.2	328	13	-13	3.0	11	9	9
4	192040	192303	14.3	328	16	-21	2.9	10	11	5

TABLE 1

Summary of T-28 Penetration Data from 11 July 1985.
(Values are maxima/minima observed for each penetration)

*Based on an assumed density of 0.9 g cm^{-3}.

The Conquest also made numerous penetrations about 1.5 km below the T-28, through low-reflectivity regions along the south side of the storm (Oleskiw and English, 1986). The initial seeding treatment (using dry ice at a "low" rate of 100 g km^{-1}) began at 1838, during the second T-28 penetration of the storm. The second treatment (using dry ice at a "high" rate of 1 kg km^{-1}) began at 1922, during the final T-28 penetration. Because of this timing, the T-28 observations can add little to the Oleskiw and English discussion of the seeding experiments, except for a more complete description of the storm initial conditions.

The largest observed hailstone sizes were >4 cm on each T-28 penetration. Both the temperatures and equivalent potential temperatures ($\theta_e \sim 330$ K) were several degrees lower than would be expected from an adiabatic ascent. This is in fairly good agreement with the cloud liquid water concentrations (LWC); the peaks tended to be about 60-70% of adiabatic, according to measurements from a Forward Scattering Spectrometer Probe (FSSP) carried on the T-28. A substantial amount of mixing may have occurred, because there were no distinct regions of high equivalent potential temperatures in the updrafts as are often found in other T-28 observations (e.g., Musil et al., 1986).

The lengths of the penetrations (L), the peak vertical wind velocities, and the turbulence values are quite typical of other T-28 penetrations in active hailstorms. The vertical velocities were similar on all penetrations, except that the updrafts were weaker on Penetration 2. The hailstone number (N_T) and

Fig. 2: Plan position indicator plot at 0.9° from the S-band Alberta radar near the time of the first T-28 penetration. Contours of equivalent radar reflectivity (dBZ) are labeled and the triangles represent reflectivities 15-20 dBZ. The tic marks on the axes are at 1-km intervals from the center of the plot located at 335°/83 km.
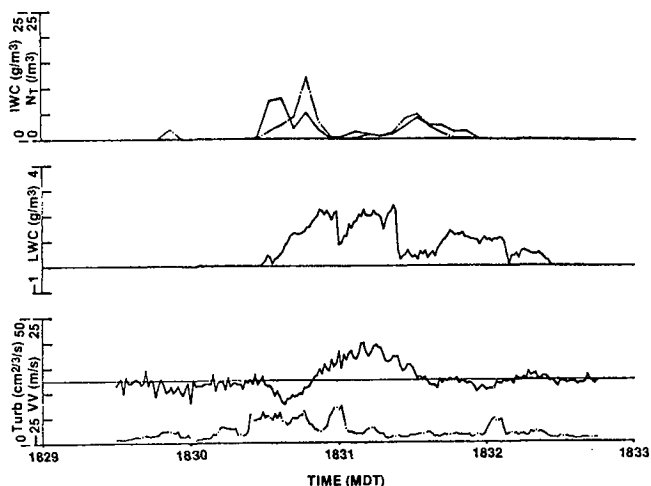
Fig. 3: Plot of T-28 data for Penetration 1 on 11 July 1985, made from southeast to northwest. Upper panel: Equivalent hail mass concentration - g m^{-3} (dash-dot), hailstone number concentration - m^{-3} (solid); middle panel: FSSP liquid water concentration - g m^{-3}; lower panel: Kopp vertical wind velocity - m s^{-1} (solid), turbulence - cm$^{2/3}$ s^{-1} (dash-dot). The time scale can be converted to an approximate distance scale using the nominal T-28 flight speed of 6 km/min.

mass (W_H) concentrations represent maxima obtained over 5-s time periods for each penetration. Penetration 2, at a time when the updrafts were relatively weak, exhibited the largest hail amounts; there was also a substantial amount of cloud water in the downdraft region on that penetration.

Figure 3 shows a sample plot of several variables for Penetration 1, which is mostly typical of the other penetrations. Included are plots of the 5-s hail mass and number concentrations along with FSSP cloud water concentration, vertical wind, and turbulence at 1-s intervals. The LWC peaks exceed 2 g m^{-3} through most of the updraft; the Conquest observed similar values at a lower altitude (4.6 km). The turbulent eddy dissipation rate exceeded 10 cm$^{2/3}$ s^{-1} over a substantial portion of the penetration. The radar data have not been analyzed with specific regard to the T-28 penetrations, so the exact orientation of these observations with respect to the reflectivity structure as shown by Oleskiw and English (1986) is not known.

Figure 4 shows a typical cloud droplet size distribution averaged over a 5-s time period near the middle of the updraft region shown in Fig. 3. The presence of large droplets is unusual in High Plains thunderstorms, but was quite common in this storm.

4. HAIL OBSERVATIONS

A detailed analysis of the T-28 data gathered on 11 July was accomplished. Of special interest are the observations of hailstones from the Institute of Atmospheric Sciences (IAS) laser shadowgraph hail spectrometer (Jansen, 1981). This instrument operates on the same basic principles as the probes described by Knollenberg
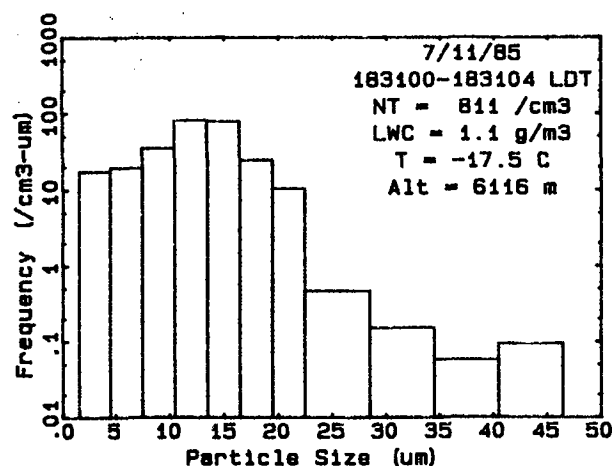
Fig. 4: Typical cloud droplet size distribution from an FSSP, observed near the middle of the updraft region shown in Fig. 3. Inset shows total droplet concentration (NT), LWC, temperature (T), and altitude (ALT).

(1981) and provides both "one-dimensional" particle size distributions and two-dimensional images (see Appendix).

4.1 Hailstone Size Distributions

The size distributions from the 1-D portion of the hail spectrometer have been summarized for each penetration on 11 July (Fig. 5) for the times when hail was present during the penetration. In Penetration 1 (Fig. 5A), reasonable images up to about 4 cm in size were also observed so that one can be confident that particles that large were present. Some of the 4-and 5-cm hailstone counts could be questionable due to the broken-up nature of some of the very large particle images; however, a "slow-particle detection" feature in the 1-D channel is designed to reject such events. In any event, the total concentrations of hailstones are not affected very much by the counts of large stones (because the high concentrations of small stones dominate that calculation).

The hailstones do not conform exactly to exponential size distributions, which would appear as straight lines on these semi-log plots. However, the pronounced kink at about 1.5 cm diameter noted in the plots by Smith and Jansen (1982) is not evident here. No attempt was made to fit any curve to the distributions.

The times shown in the insets of Fig. 5 indicate the times when hail was observed during each penetration. The hail was continuous during that entire period, although the concentrations fluctuated a great deal within the interval. The time interval in Fig. 5A corresponds to a hail region approximately 9 km across, which is a relatively large region of continuous hail in comparison to past T-28 observations. The hail regions on subsequent penetrations were even wider.

The largest region of hail, about 14 km across, occurred during Penetration 3 (Fig. 5C), although more hailstones were found in Penetration 2. Thus, the average total number
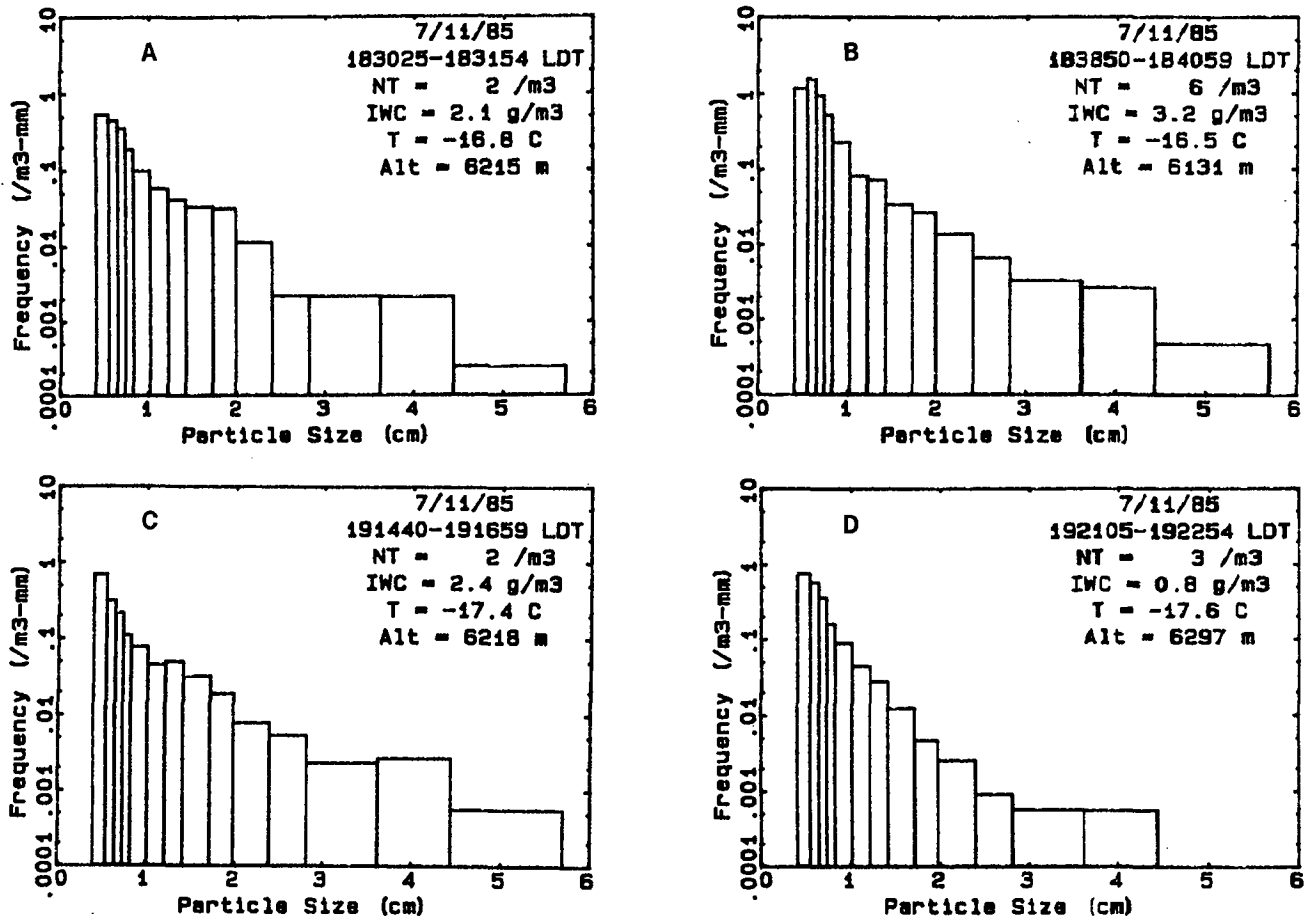
Fig. 5: Composite hailstone size distribution for each penetration on 11 July 1985 from 3-s portions of hail spectrometer. Inset indicates time when hail was observed and averages for total concentration (NT), equivalent hail mass concentration (IWC), temperature (T), and altitude (ALT) for that period. Ordinate has units of m^{-3} mm^{-1} of size interval. A, B, C, D correspond to penetrations 1-4, respectively.

concentration (N_T) and equivalent ice mass concentration (IWC) were greatest in Penetration 2. No specific physical reasons for the higher values are known, but the flight track for Penetration 2 carried the aircraft through higher reflectivity regions north and east of the strong updraft region. The coexistence of significant hail and supercooled cloud water in a moderate downdraft on that penetration may have signified an enhanced growth environment at the time. Penetrations 3 and 4 had size distributions that were more similar to those found in Penetration 1.

The mass concentrations were calculated assuming that the particles had a density of 0.9 g cm^{-3}, leading to average IWC values ranging between about 1-3 g m^{-3}. These mass concentrations are somewhat higher than those found by other investigators (e.g., Heymsfield, 1978). On the average, Heymsfield's calculations result in hailstone masses 20-30% lower than those obtained assuming a constant density of 0.9. The differences are even greater for the smaller sizes, where Heymsfield's method may be more correct because the observed densities there are typically lower than 0.9 g cm^{-3} (Knight and Heymsfield, 1983).

4.2 Hail Locations

Hailstone size distributions were also determined for 5-s time periods for each penetration. From these distributions, values of N_T and IWC have been calculated as a function of time (see Fig. 3) to permit an analysis of the locations of the hail in relation to some of the other T-28 measurements. The observed locations of the hail may be related partly to the path of the T-28 through the storm, because the penetrations did not pass through exactly the same portion of the storm in each case.

In Penetration 1, the largest amounts of hail were found near the edges of the updraft region and in the adjacent downdraft regions. This is similar to the common situation in other hailstorms of the High Plains (e.g., Sand, 1976). There was some hail throughout nearly the entire LWC region, which in turn extended well beyond the updraft. The subsequent penetrations tended not to show larger amounts of hail near the updraft edges, but the coexistence of hail and supercooled cloud water was typical of all the penetrations. On Penetration 2, most of the hail was in a downdraft containing up to 2 g m^{-3} of cloud liquid.

5. HAIL GROWTH PROCESSES

The observations discussed in the foregoing section indicate that the hailstones encountered were still growing, because they were predominantly found in regions with supercooled cloud water. In fact, when one compares the mass of

hail which was accreting cloud liquid to the total mass of hail found in each penetration, nearly 100% of the hail was still in a favorable growth environment when encountered by the T-28.

5.1 Hailstone Motions

No Doppler data were available in this project, so it was only possible to study hailstone trajectories in this storm by examining the fine-scale reflectivity patterns (as in Oleskiw and English, 1986). Their findings suggest parcel trajectories that would carry particles from cumulus turrets on the south edge of the storm right through the regions of the storm penetrated by the T-28. However, information about the vertical motions is limited.

A simple comparison of hailstone terminal velocities (V_t) with the vertical winds from the T-28 measurements provides useful information about vertical hailstone motions in the cloud. The comparison was accomplished by determining which of the observed hailstones were rising or falling in the vertical-wind environment measured by the T-28. Figure 6 shows a plot of the largest hail size observed in each 5-s time period during Penetration 1, as well as the maximum-sized hailstone that would just be balanced in the vertical wind field at that time. Whenever the "balance" curve (dashed) exceeds the maximum hail size observed, all the observed hail is rising in the updraft; when it is below the maximum-size curve, only the hailstones smaller than the sizes indicated by the "balance" curve are rising. In all other locations, all the hail is descending in downdraft air. Overall, the region of rising hail (which, of course, is located in the updraft region - compare with Fig. 3) is very small compared to the total amount of observed hail. However, even in the updraft region there are hailstones which are descending, except for a small region near 1831 MDT in the plot.
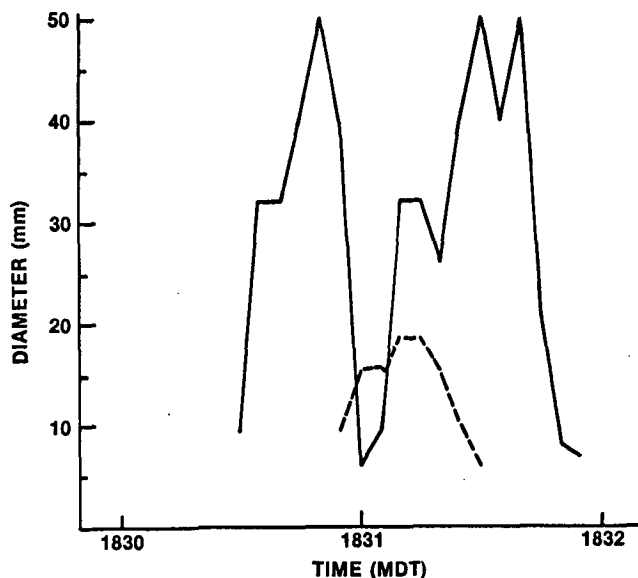
Fig. 6: Distribution of hail sizes vs. time for 5-s time periods for Penetration 1 on 11 July 1985. Solid line shows maximum-sized hail, while dashed line shows maximum-sized hail that would just be balanced in the observed updrafts.

In terms of mass of hail, the amount rising was small for all the penetrations, ranging from <1% on Penetration 2 to a maximum of about 20% on Penetration 4. In other words, while most of the hail was growing when observed (because of its coexistence with cloud liquid water), most of it was also descending, even in the updrafts at the T-28 penetration altitudes.

The comparisons in the preceding paragraphs should be considered estimates because in comparing calculated terminal velocities and vertical winds from the T-28 data, we are dealing with quantities involving substantial uncertainties. Knight and Heymsfield (1983) made calculations of V_t for hailstones falling near the ground and Heymsfield (1978) developed a set of empirical equations for various types and sizes of hydrometeors. Some models of particle growth have used a variable-density technique for dealing with particle terminal velocities in Doppler flow fields (e.g., Heymsfield, 1982; Foote, 1984). Other numerical investigations (Musil, 1970; Dennis and Musil, 1973; Nelson, 1983) have assumed a hailstone density of about 0.9 g cm^{-3} for calculating terminal velocities for hailstones greater than 1 cm diameter. This results in terminal velocities substantially greater than those reported by the other investigators. However, precise calculations are not possible because little is known about the terminal velocities of actual hailstones in atmospheric free fall, especially at mid-storm levels. Because at least some observations tend to show lower terminal velocities, especially for the smaller hydrometeors, and knowledge of the subject is limited anyway, we used the Heymsfield (1978) empirical equations for estimating V_t. This contrasts with the assumption of a fixed density used in calculating the hail mass concentrations, and is intended to produce conservative estimates of the terminal velocities. If a hailstone density of 0.9 g cm^{-3} had been assumed, the regions of rising hail would have been even smaller than shown in Fig. 6. Kopp (1985) discusses the uncertainties in the vertical-wind calculations.

Although the hailstones found in downdraft regions will continue to grow as long as they coexist with supercooled liquid water, the hail (along with the smaller ice hydrometeors) will likely deplete the liquid rather quickly in those regions. Depletion calculations have not been made with this data set, but the depletion equations used by Heymsfield and Musil (1982) suggest that it could be accomplished in something of the order of two minutes in the downdraft regions. Evaporation effects are unknown, but would only accomplish the depletion faster.

Most of the hailstones in the downdraft regions therefore were probably nearing the end of their growth cycle, as the updraft appeared to be essentially vertical. Those found in or at the edges of the updraft regions would have the best opportunity to continue growing because there was an ample supply of cloud liquid that was continually being replenished. There is a strong suggestion in these data that a substantial amount of hail growth had occurred at altitudes above the T-28 since many hailstones were already very large when observed by the T-28.

183101

183102

183104

183105

Fig. 7: Sample of 2D-C images near the middle of the updraft region (~ 1831 MDT) shown in Fig. 3. Vertical bars approximately 1 mm long.

5.2 Hailstone Growth Regime and Embryo Sources

The growth modes of the hailstones observed in this storm were investigated by computing the wet and dry growth rates for a wide variety of hailstone sizes, cloud liquid water concentrations, and temperatures. The calculations of dry and wet growth regimes follow the work by Musil (1970) and Dennis and Musil (1973). Small ice particles were also considered in these calculations and were found to be an important factor. A sample of the particles measured with a 2D-C probe near the middle of the updraft region in Fig. 3 is shown in Fig. 7. They range from hundreds of micrometers to several millimeters in size. The related mass concentrations are unknown, but 1 g m^{-3} was taken as a typical value (Knight and Squires, 1982) for the growth-regime investigation. The presence of small ice particles allows the hailstones to remain in a dry growth regime somewhat longer than would otherwise be, because the accreted ice tends to keep the hailstones cooler.

Figure 8 is a sample plot showing the boundaries between dry and wet growth regimes for conditions near those found on 11 July. The area to the left of each curve indicates the dry growth region and the area to the right, the wet growth region for the corresponding conditions. The dashed line outlines the approximate region of the bulk of the hailstone observations on 11 July.

The vast majority of the observed hailstones fall within the dry growth regime, which is not surprising considering the low temperatures of the T-28 penetrations. As the hailstones fall, however, they likely increase somewhat in size and the dry/wet growth boundary also moves to the left (as suggested by the curve for -5°C in Fig. 8). Thus, lower in the cloud, the wet growth process should be active, and could produce raindrops by shedding. As descending hailstones were found in the updraft regions, the shed drops could provide a source of frozen-drop embryos for subsequent hailstone development. This has been noted as a significant embryo source in at least some High Plains hailstorms (e.g., Rasmussen and Heymsfield, 1987).

The present calculations cannot say anything about the possible development of embryos in other regions of the cloud. The observations reported by Oleskiw and English (1986) showed embryo-size ice particles appearing lower down in cumulus turrets on the southern edge of the storm. Millimeter-sized particles appeared so quickly that it seems likely they were generated in a different part of the storm. The observed storm-relative winds and the fine-scale reflectivity pattern analysis showed that these particles could be transported into the main part of the storm to act as hail embryos. This and the shedding process could therefore provide a combination of graupel and frozen-drop embryos, through recirculation processes which cannot yet be specified in detail.

Frozen-drop embryos could also result from the melting of hail once it has fallen below the melting level, with recirculation of the resulting drops into the updraft (e.g., Heymsfield and Hjelmfelt, 1984). It is not known whether the embryos in this storm were predominantly graupel or frozen drops; both types have been found in hailstones from other Alberta storms (Knight, 1981). However, it appears that some type of recirculation mechanism must be involved in either case, since it is unlikely that much of the hail observed by the T-28 could be developed in a single simple up-and-down trajectory.

Fig. 8: Plot showing boundary between regions of dry and wet growth of hailstones, for temperatures of -17°C with an LWC of 1 g m^{-3} and -5°C with no ice. Dry growth region is to left of boundary, wet growth region to right. Area enclosed by dashed line defines approximate region of most of the hailstone observations with the T-28 on 11 July 1985.

Further investigation of the embryo question is necessary and it is planned to explore this with the aid of comparisons of T-28 and other observations with numerical cloud model output. The approach will be similar to that accomplished by Kubesh et al. (1988) for a storm in southeastern Montana.

6. SUMMARY OF RESULTS

The data gathered by the T-28 on 11 July 1985 provided valuable in situ observations from an isolated Alberta hailstorm. This permitted an analysis of some of the characteristics of the hailstone distributions in this storm in relation to other T-28 measurements. These characteristics, as well as the vertical winds and cloud LWC, were generally similar to past observations by the T-28 in other High Plains storms. However, hail was observed over larger regions of each penetration on 11 July than is usual in other locations where the T-28 has operated. The data also included the first 2-D images of hailstones from the hail spectrometer in flight.

Even though the analysis of the data is incomplete, a preliminary assessment of the hail growth mechanisms in this storm has been made. The hail was almost always found in relatively high concentrations of supercooled cloud water, on the order of 1-2 g m^{-3}, indicating that the hail was still growing at the time of observation. Most of the observed hailstones at the -17°C level were growing in a dry growth regime, as well as descending in the cloud. A wet growth process was likely active lower in the storm. There are strong indications that the hail achieved a substantial portion of its growth above the T-28 altitudes. Recirculation of particles probably played a significant role in the hail mechanism because it is unlikely that the hail sizes observed by the T-28 could have resulted from a single trip through the cloud. It is not known what role the cumulus towers to the southwest may have played in providing hail embryos for this storm.

Additional work is necessary to combine the FSSP, 2D-C probe, foil impactor, and hail spectrometer data in order to examine the total hydrometeor spectra measured by the T-28 in this storm. Further information about the hail mechanism could then be obtained by making comparisons between the aircraft observations and the results of 2D time-dependent model simulations for both bulk water and hail-category microphysics (e.g., Farley, 1987). Detailed analysis of the radar history of this storm would also aid in such an investigation.

7. REFERENCES

Dennis, A. S., and D. J. Musil, 1973. Calculations of hailstone growth and trajectories in a simple cloud model. J. Atmos. Sci., 30:278-288.

English, M., 1986. The testing of hail suppression hypotheses by the Alberta Hail Project. Preprints 10th Conf. Wea. Modif., Arlington, VA, Amer. Meteor. Soc., 72-76.

Farley, R. D., 1987. Numerical modeling of hailstorms and hailstone growth. Part III: Simulation of an Alberta hailstorm -- natural and seeded cases. J. Climate Appl. Meteor., 26:789-812.

Foote, G. B., 1984: A study of hail growth utilizing observed storm conditions. J. Climate Appl. Meteor., 23:84-101.

_____, and H. W. Frank, 1983. Case study of a hailstorm in Colorado. Part III. Airflow from triple-Doppler measurements. J. Atmos. Sci., 40:686-707.

Heymsfield, A. J., 1978. The characteristics of graupel particles in northeastern Colorado cumulus congestus clouds. J. Atmos. Sci., 35:284-295.

_____, 1982. A comparative study of the rates of development of potential graupel and hail embryos in High Plains storms. J. Atmos. Sci., 39:2367-2897.

_____, and M. R. Hjelmfelt, 1984. Processes of hydrometeor development in Oklahoma convective clouds. J. Atmos. Sci., 41:2811-2835.

_____, and D. J. Musil, 1982. Case study of a hailstorm in Colorado. Part II: Particle growth processes at mid-levels as deduced from the in-situ measurements. J. Atmos. Sci., 39:2847-2866.

Humphries, R. G., M. English and J. Renick, 1987. Weather modification in Alberta. J. Wea. Modif., 19:13-24.

Jansen, D. C., 1981. An analysis of airborne hail spectrometer data. M.S. Thesis, Department of Meteorology, South Dakota School of Mines and Technology, Rapid City, SD. 83 pp.

Johnson, G. N., and P. L. Smith, Jr., 1980. Meteorological instrumentation system on the T-28 thunderstorm research aircraft. Bull. Amer. Meteor. Soc., 61:972-979.

Knight, C. A., and P. Squires (eds.), 1982. Hailstorms of the Central High Plains. Vol. I: The National Hail Research Experiment. Colorado Associated University Press, Boulder, Colorado. 282 pp.

Knight, N. C., 1981. The climatology of hailstone embryos. J. Appl. Meteor., 20:750-755.

_____, and A. J. Heymsfield, 1983. Measurement and interpretation of hailstone density and terminal velocity. J. Atmos. Sci., 40:1510-1516.

_____, A. J. Weinheimer and M. B. Steiner, 1986. The use of powdered iron as a tracer in hailstorm research. Preprints Joint Sessions 23rd Conf. Radar Meteor. and Conf. Cloud Physics, Snowmass, CO, Amer. Meteor. Soc., JP1-JP2.

Knollenberg, R. G., 1981. Techniques for probing cloud microstructure. In Clouds, Their Formation, Optical Properties, and Effects. (P. V. Hobbs and A. Deepak, eds.). Academic Press, NY. 497 pp.

Krauss, T. W., and J. D. Marwitz, 1984. Precipitation processes within an Alberta supercell hailstorm. J. Atmos. Sci., 41:1025-1034.

Kubesh, R. J., D. J. Musil, R. D. Farley and H. D. Orville, 1988. The 1 August 1981 CCOPE storm: Observations and modeling results. J. Appl. Meteor., 27:216-243.

Musil, D. J., 1970. Computer modeling of hailstone growth in feeder clouds. J. Atmos. Sci., 27:474-482. [Reply: J. Atmos. Sci., 28:294-295]; [Corrigendum: J. Atmos Sci., 29:225].

_____, A. J. Heymsfield and P. L. Smith, 1986. Microphysical characteristics of a well-developed weak echo region in a High Plains supercell thunderstorm. J. Climate Appl. Meteor., 25:1037-1051.

Nelson, S. P., 1983. The influence of storm flow structure on hail growth. J. Atmos. Sci., 40:1965-1983.

Oleskiw, M. M., and M. English, 1986. A comparison of several seeding treatments on growing towers within Alberta hailstorms. Preprints 10th Conf. Wea. Modif., Arlington, VA, Amer. Meteor. Soc., 84-89.

Rasmussen, R. M., and A. J. Heymsfield, 1987. Melting and shedding of graupel and hail. Part III: Investigation of the role of shed drops as hail embryos in the 1 August CCOPE severe storm. J. Atmos. Sci., 44:2783-2803.

Sand, W. R., 1976. Observations in hailstorms using the T-28 aircraft system. J. Appl. Meteor., 15:641-650.

Smith, P. L., and D. C. Jansen, 1982. Observations inside SESAME thunderstorms with an airborne hail spectrometer. Preprints 12th Conf. Severe Local Storms, San Antonio, TX, Amer. Meteor. Soc., 16-19.

_____, D. J. Musil and D. C. Jansen, 1980. Observations of anomalous large particles inside Colorado and Oklahoma thunderstorms. Proc. VIII Intnl. Conf. Cloud Physics, Clermont-Ferrand, France, 295-298.

APPENDIX: IMAGING CAPABILITY IN THE HAIL SPECTROMETER

For many years, the hail spectrometer aboard the T-28 has provided one-dimensional size data, with 14 size categories ranging from about 0.5-5 cm in diameter. Although these data have been useful and of apparent good quality, there have often been questions about the very large particles observed during the T-28 penetrations (Smith et al., 1980). The possibility of contamination due to ice fragments shedding from leading edges of the aircraft wing or the forward portion of the spectrometer could not readily be discounted.

To help resolve these questions, an imaging system working in conjunction with the 1-D categorization scheme was developed. The imager scans the array of 64 laser-illuminated phototransistors every 10 µs whenever a shadow is present in the array, thereby producing an image slice for about every millimeter of aircraft travel. (Only every other sensor in the 1-D array is scanned, so the image resolution across the array is about 1.8 mm.) The resultant 64-bit slice is compressed into a 16-bit word and stored in a buffer prior to being recorded on magnetic tape.

During the summer of 1985, images of significant hail encounters were obtained for the first time. Several buffers of images from the hail spectrometer during Penetration 1 (~1831 MDT) on 11 July are shown in Fig. A1. Good images are readily apparent, some as large as 2-3 cm in diameter. Also evident are some extremely large images which may be a result of shedding from the forward portion of the hail spectrometer. Most of these appear to be causing a data overflow problem, so that the images appear partially broken up. A "slow-particle detection" feature in the 1-D channel should reject such images from being counted. A weak intermittent detector is also evident, as indicated by the nearly continuous signal occurring at times near the middle of some buffers.

Generally, the spectrometer performed well in Alberta, but image data of consistently usable quality were not obtained. Many of the characteristics of hailstone size distributions are adequately represented by the 1-D portion of the hail spectrometer data. Following these initial observations, modifications have been made to the hail spectrometer imaging electronics, but no flight tests in sizable hail have yet been made.
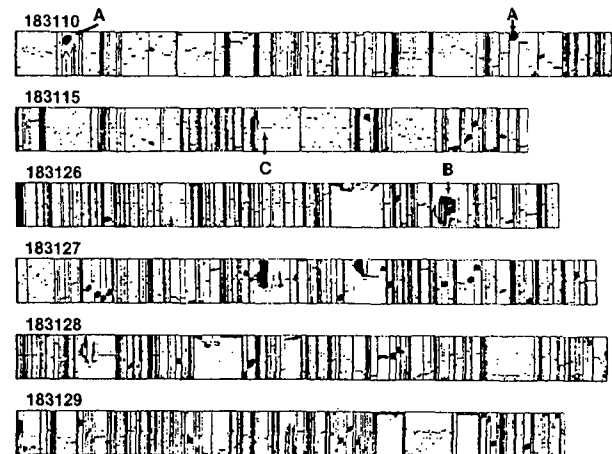
Fig. A1: Dump of several image buffers from hail spectrometer between 183110-183129 MDT on 11 July 1985. Width of array (vertical bars) about 12 cm. (A) Image > 3 cm diameter; (B) Shed broken-up image; (C) Weak intermittent diode malfunction.